PCCP

Cite this: *Phys. Chem. Chem. Phys.*, 2011, **13**, 19632–19640

www.rsc.org/pccp

PAPER

Ultrafast photoinduced relaxation dynamics of the indoline dye D149 in organic solvents†

Peter W. Lohse,[a] Julia Kuhnt,[b] Sergey I. Druzhinin,[a] Mirko Scholz,[b] Maria Ekimova,[a] Torsten Oekermann,[c] Thomas Lenzer*[a] and Kawon Oum[a]

Received 27th July 2011, Accepted 21st September 2011
DOI: 10.1039/c1cp22429h

The relaxation dynamics of the indoline dye D149, a well-known sensitizer for photoelectrochemical solar cells, have been extensively characterized in various organic solvents by combining results from ultrafast pump–supercontinuum probe (PSCP) spectroscopy, transient UV-pump VIS-probe spectroscopy, time-correlated single-photon counting (TCSPC) measurements as well as steady-state absorption and fluorescence. In the steady-state spectra, the position of the absorption maximum shows only a weak solvent dependence, whereas the fluorescence Stokes shift $\Delta\tilde{\nu}_F$ correlates with solvent polarity. Photoexcitation at around 480 nm provides access to the S_1 state of D149 which exhibits solvation dynamics on characteristic timescales, as monitored by a red-shift of the stimulated emission and spectral development of the excited-state absorption in the transient PSCP spectra. In all cases, the spectral dynamics can be modeled by a global kinetic analysis using a time-dependent S_1 spectrum. The lifetime τ_1 of the S_1 state roughly correlates with polarity [acetonitrile (280 ps) < acetone (540 ps) < THF (720 ps) < chloroform (800 ps)], yet in alcohols it is much shorter [methanol (99 ps) < ethanol (178 ps) < acetonitrile (280 ps)], suggesting an appreciable influence of hydrogen bonding on the dynamics. A minor component with a characteristic time constant in the range 19–30 ps, readily observed in the PSCP spectra of D149 in acetonitrile and THF, is likely due to removal of vibrational excess energy from the S_1 state by collisions with solvent molecules. Additional weak fluorescence in the range 390–500 nm is observed upon excitation in the $S_0 \rightarrow S_2$ band, which contains short-lived $S_2 \rightarrow S_0$ emission of D149. Transient absorption signals after excitation at 377.5 nm yield an additional time constant in the subpicosecond range, representing the lifetime of the S_2 state. S_2 excitation also produces photoproducts.

1. Introduction

Indolines have emerged as an important class of metal-free sensitizer dyes for photoelectrochemical solar cells, in which they replace standard ruthenium-based complexes, which are more expensive and also have absorption coefficients which are lower by a factor of five.[1–9] They have been proven to be especially useful in ZnO-based dye-sensitized solar cells, where the typical ruthenium complexes developed for the sensitization of TiO_2 cannot be used, since they tend to etch the ZnO surface and form aggregates on it.[10–13] To achieve a better overlap with the solar spectrum, a range of structurally modified indoline dyes with an increasing red-shift of the absorption spectrum have been synthesized.[1–3] One of the most frequently used indolines for solar-cell applications is D149, which is depicted in Fig. 1. Surprisingly, so far there has been only very limited information on indoline dynamics after photoexcitation, *e.g.*, a study of Fakis *et al.* for D149 in toluene and acetonitrile and on Al_2O_3 and TiO_2 surfaces using single-wavelength fluorescence up-conversion,[14] which will be discussed with respect to our current findings below. In addition, DFT/TD-DFT calculations have been reported and assigned considerable charge transfer (CT) character to the S_1 state.[15,16]

Here we present a comprehensive investigation of D149 in various organic solvents using ultrafast transient absorption spectroscopy, time-correlated single-photon counting (TCSPC) measurements as well as steady-state absorption and

[a] *Universität Siegen, Physikalische Chemie, Adolf-Reichwein-Str. 2, 57076 Siegen, Germany. E-mail: lenzer@chemie.uni-siegen.de; Fax: +49 271 740 2805; Tel: +49 271 740 2803*
[b] *Georg-August-Universität Göttingen, Institut für Physikalische Chemie, Tammannstr. 6, 37077 Göttingen, Germany*
[c] *Institut für Physikalische Chemie und Elektrochemie, Leibniz-Universität Hannover, 30167 Hannover, Germany*

† Electronic supporting information (ESI) available: Results of photostability experiments using sub-400 nm excitation in the $S_0 \rightarrow S_2$ band of D149 in ethanol solution by cw lamp illumination. See DOI: 10.1039/c1cp22429h

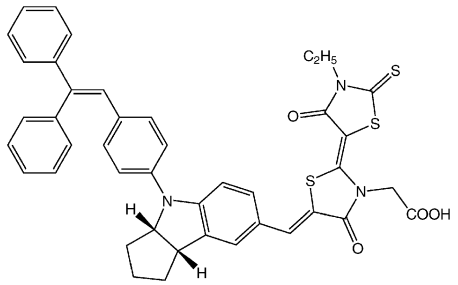

Fig. 1 Chemical structure of indoline D149 (adapted from ref. 6).

fluorescence. After S_1 excitation, the photoinduced dynamics of this sensitizer dye appear to be fairly simple, despite its rather complicated structure. In contrast, the dynamics after S_2 excitation turn out to be much more complex and point toward the additional formation of photoproducts.

2. Experimental

2.1 Pump–supercontinuum probe (PSCP) spectroscopy

A detailed description of PSCP spectroscopy was already given elsewhere,[17] and here we only briefly discuss the setup used in our experiments:[18–20] a regenerative Ti:Sa system (Spectra-Physics Hurricane, center wavelength: 780 nm, repetition rate: 920 Hz, pulse length: 100 fs, 1 mJ pulse^{-1}) was employed for pumping two home-built NOPAs.[21,22] The pump NOPA generated pulses centered at 476–484 nm, which were compressed by a pair of quartz prisms and then attenuated by pellicle beam splitters to excite D149 *via* its $S_0 \rightarrow S_1$ transition (photon density *ca.* 5×10^{14} cm^{-2}). The second NOPA generated a wavelength of *ca.* 550 nm which was also compressed by a quartz prism pair and then focused into a 1 mm thick calcium fluoride plate generating a multifilament supercontinuum, where the range 340–770 nm was used in the current study. The supercontinuum was spectrally filtered by a dye solution and then split up into reference and sample beams. Pump and probe pulses were overlapped at magic-angle polarization in a stainless steel flow cell with 400 μm path length and 200 μm thick quartz windows. Reference and sample spectra were dispersed by two spectrographs with 512 element photodiode arrays. Transient spectra for each pump–probe delay represent the average of three independent scans, each consisting of 500 laser shots employing single-shot baseline correction. Solvent signals arising during the cross-correlation time were not subtracted from the experiment signals, and can be easily discerned by their characteristic time dependence. The pump–probe intensity cross-correlation time in the current experiments was 90–100 fs and the time accuracy 10 fs.

2.2 UV pump–VIS probe transient absorption spectroscopy

Details of this setup can be found in previous publications,[23,24] and here we focus only on the specifics relevant for the current experiments: the output of a mode-locked Ti:sapphire oscillator (Spectra-Physics Tsunami, 80 MHz; pump source: Spectra-Physics Millenia Xs Nd:YVO_4 laser) generated red pulses at 755 nm with an average power of 1.2 W. The laser beam was split into two parts. One beam traversed an acousto-optic modulator (AOM, 2 MHz modulation frequency) with subsequent frequency-doubling in an LBO crystal, resulting in an intensity-modulated UV pump beam (377.5 nm, pulse energy < 0.1 nJ). The other part had a typical energy <1 nJ pulse^{-1} and was directly used as a probe beam (755 nm). The time resolution of the setup was *ca.* 130 fs. Pump and probe pulses at magic-angle polarization were collinearly recombined and focused into a quartz flow cuvette containing D149 in the solvent of interest. Transient absorption was detected by an avalanche photodiode using an appropriate set of cut-off filters for the pump beam wavelength. The signal was processed by a lock-in amplifier which used the same 2 MHz reference as the AOM.

2.3 Nanosecond time-correlated single photon counting (TCSPC)

The basic setup of the TCSPC system was described before.[25,26] In the current measurements, a solution of D149 in THF, acetonitrile or chloroform (OD 0.3) was excited by a pulsed N_2 flash lamp (FWHM 2 ns) at a repetition rate of 50 kHz. The unpolarized radiation of the N_2 line at 337 nm was selected by a monochromator (Jobin-Yvon H.20 UV, bandwidth: 1–2 nm) and emission was detected at the maximum of the fluorescence spectrum using an identical monochromator combined with a photomultiplier (Philips XP2020). The signal was fed into a time-to-amplitude converter (Tennelec TC 862) connected to a multi-channel analyzer (Silena ADC 7423 UHS). A scatter solution (Ludox, Du Pont) and the D149 sample solution were alternately translated into the excitation beam until 1000 counts in the maximum were accumulated. Decay curves were deconvolved with the instrument response function (IRF) resulting in mono-exponential decays. With this setup, single exponential decay time constants down to a few hundred ps can be determined.

2.4 Steady-state absorption and fluorescence

Absorption spectra were recorded on Varian Cary 5E and 5000 spectrometers with baseline correction. Fluorescence spectra were detected using Horiba Jobin-Yvon Fluorolog-3 and Varian Cary Eclipse spectrometers. Fluorescence raw data were corrected for the instrument response function.

2.5 Photostability experiments in the UV

For photostability measurements in the $S_0 \rightarrow S_2$ band of D149 below 400 nm, the light from a cw high-pressure Hg–Xe lamp (Osram HBO, 200 W) was passed through an appropriate set of optical glass filters (Schott UG1 and WG320) and mildly focused into the sample cuvette (10 mm × 10 mm) by a quartz lens ($f = 150$ mm) at an angle of 90° with respect to the beam path of the absorption spectrometer. The resulting power density at the sample was *ca.* 50 mW cm^{-2}.

2.6 Chemicals

The indoline dye D149 was purchased from Inabata UK Ltd. and used without further purification. Solvents had a specified purity of 99% or better. The absorption, fluorescence and TCSPC measurements were carried out at 298 K in nitrogen saturated solution. We note that solutions of D149 in acetonitrile showed absorption shifts in the nm range and sometimes formation of a weak blue shoulder, which are tentatively

assigned to a side-reaction of D149, possibly with O_2 or aggregate formation.

3. Results and discussion

3.1 Steady-state absorption and fluorescence of D149

Steady-state absorption and fluorescence spectra in six organic solvents are depicted in Fig. 2. Characteristic values are summarized in Table 1 including the polarizability $R(n) = (n^2 - 1)/(n^2 + 2)$ and the polarity function $\Delta f = R(\varepsilon) - R(n) = (\varepsilon - 1)/(\varepsilon + 2) - (n^2 - 1)/(n^2 + 2)$, calculated from tabulated n and ε values.[27] The absorption spectra show only a weak solvent dependence. They consist of two bands centered at 530 nm and 390 nm, which correspond to the $S_0 \rightarrow S_1$ and $S_0 \rightarrow S_2$ transitions, respectively (slightly shifted in chloroform).

The fluorescence spectra were obtained after excitation at the maximum of the $S_0 \rightarrow S_1$ absorption band. They exhibit a substantial Stokes shift $\Delta\tilde{\nu}_F$, which is correlated with solvent polarity (*e.g.* 2780 cm^{-1} in chloroform compared to 4050 cm^{-1} in acetonitrile), indicating that the dipole moment of D149 increases upon photoexcitation, see also Table 1. We note that Fakis *et al.*[14] reported the fluorescence maximum in acetonitrile at *ca.* 615 nm, which is blue-shifted by 49 nm with respect to our value. This large difference is likely due to a missing correction of their fluorescence spectrum with respect to detector sensitivity. Similarly, a previous study of Le Bahers *et al.*[16] reports the S_1 emission maximum in methanol at 644 nm compared to the 670 nm found in our study. The difference of 26 nm and the additional shoulder on the red side of their fluorescence spectra also suggest a missing correction for detector sensitivity in that study. A similar explanation might hold for chloroform, where Dentani *et al.* find the fluorescence maximum at 636 nm,[8] whereas our value is 643 nm.

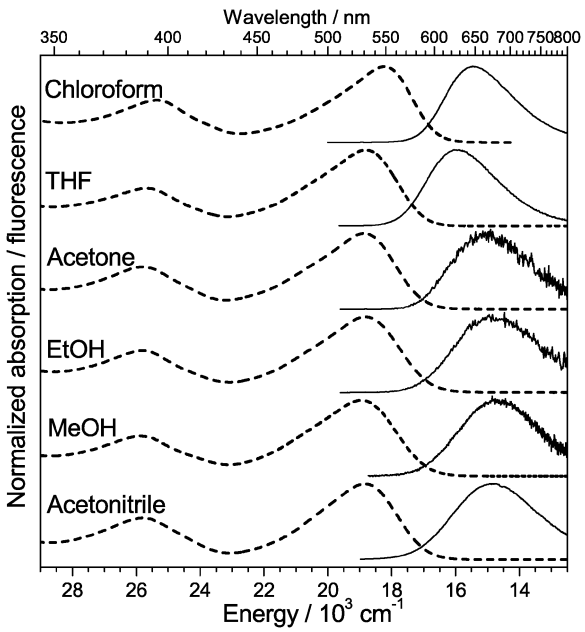

Fig. 2 Absorption spectra (dashed lines) and fluorescence spectra (solid lines) of D149 in different organic solvents. Fluorescence spectra were recorded after excitation at the absorption maximum of the $S_0 \rightarrow S_1$ band in each case.

Fig. 3(A) contains $S_1 \rightarrow S_0$ steady-state fluorescence spectra of D149 in acetonitrile and THF recorded after $S_0 \rightarrow S_1$ excitation at 487 and 522 nm (dotted lines), respectively, and $S_0 \rightarrow S_2$ excitation at 380 nm (solid lines) for D149 in both solvents. After S_2 excitation, we observe a slight red-shift of 130 and 50 cm^{-1} for the fluorescence in acetonitrile and THF, respectively. Possible reasons for this discrepancy will be discussed in Section 3.4. As can be seen from Fig. 3(B), the fluorescence spectra after S_2 excitation show an additional weak pedestal which starts to rise around 26 000 cm^{-1}. It is rather flat and merges with the S_1 emission. We note that this result is in contrast to Fakis *et al.*, who observed two distinct emission bands with a dip at *ca.* 530 nm, which were assigned to separate S_1 and S_2 emissions.[14] The pedestals in Fig. 3(B) can be assigned to weak $S_2 \rightarrow S_0$ emission, but contributions from an impurity are probably dominant (see Section 3.4). We note that the $S_2 \rightarrow S_0/S_1 \rightarrow S_0$ emission band ratio, which we obtained after deconvolution, is much smaller than in the spectra reported by Fakis *et al.*,[14] which also suggest a missing correction for detector sensitivity in their experiments. The extremely weak $S_2 \rightarrow S_0$ emission already points toward a very short lifetime of the S_2 state. Note also that the $S_2 \rightarrow S_0/S_1 \rightarrow S_0$ emission band ratio in acetonitrile is larger than in THF. We will discuss the resulting implications for the S_2/S_1 lifetime ratio in more detail in Section 3.4.

3.2 Transient PSCP spectra and TCSPC experiments

Ultrafast transient broadband absorption spectra $\Delta OD(t)$ of D149 in acetonitrile, methanol and THF are shown in Fig. 4–6, respectively. D149 was excited to the S_1 state at 476 nm (acetonitrile), 479 nm (methanol) and 484 nm (THF). Table 2 contains a summary of experimental conditions and kinetic information extracted from the PSCP spectra, including

Table 1 Characteristics of solvent dependent D149 steady-state absorption and fluorescence spectra ($S_0 \rightarrow S_1$ transition)

Solvent	$R(n)^a$	Δf^a	$\lambda^{Abs.}_{max.}$/nm	$\tilde{\nu}^{Abs.}_{max.}$/$cm^{-1}$	$\lambda^{Fl.}_{max.}$/nm	$\tilde{\nu}^{Fl.}_{max.}$/cm^{-1}	$\Delta\tilde{\nu}_F = (\tilde{\nu}^{Abs.}_{max.} - \tilde{\nu}^{Fl.}_{max.})$/$cm^{-1}$
Acetonitrile	0.212	0.711	529	18 920	664	14870	4050
Methanol	0.203	0.711	528	18 950	670	14690	4260
Ethanol	0.221	0.669	531	18 820	664	14800	4020
Acetone	0.218	0.651	530	18 870	659	15010	3860
THF	0.246	0.439	531	18 830	621	15960	2870
Chloroform	0.267	0.293	549	18 230	643	15450	2780

[a] $\Delta f = R(\varepsilon) - R(n)$, where $R(\varepsilon) = (\varepsilon - 1)/(\varepsilon + 2)$ and $R(n) = (n^2 - 1)/(n^2 + 2)$ with the dielectric constant ε and the index of refraction n of the solvent.

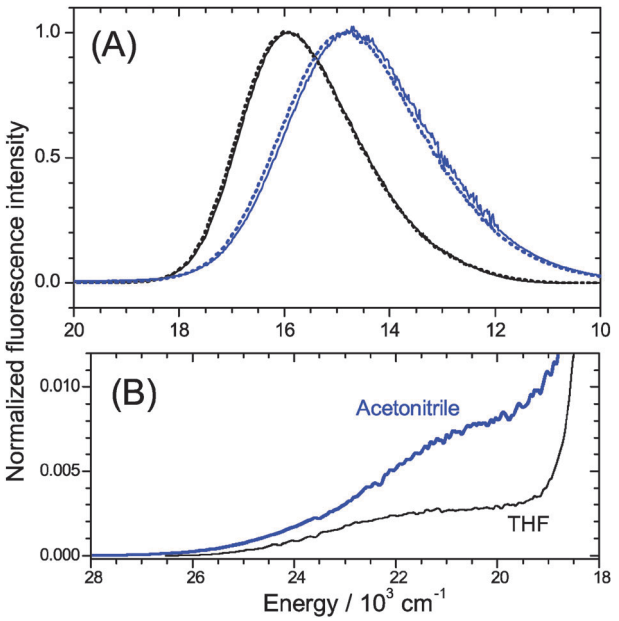

Fig. 3 (A) Steady-state fluorescence spectra of D149 after $S_0 \rightarrow S_1$ (dotted lines) and $S_0 \rightarrow S_2$ (solid lines) excitation for THF (black) and acetonitrile (blue). (B) Magnification of the fluorescence spectra after $S_0 \rightarrow S_2$ excitation shown in (A) in the region where $S_2 \rightarrow S_0$ emission is expected. Spectra in (A) below 11 800 cm^{-1} have been extrapolated.

estimated errors from the fitting procedures. A global kinetic analysis will be presented in Section 3.3.

We commence with the PSCP experiments for acetonitrile (Fig. 4): the upper plot shows the early-time dynamics between −0.1 and 0.22 ps in steps of 40 fs. Here, one observes the negative ground state bleach (GSB, $S_0 \rightarrow S_n$) of D149, with a characteristic double peak structure resembling the inverted steady-state absorption spectrum (shown as a dashed blue line in the bottom panel). In addition, nascent stimulated emission (SE) is visible to the red of the GSB, arising from the S_1 state prepared by photoexcitation. It is superimposed by weaker structured Raman contributions, which disappear as soon as the pump and probe pulses no longer overlap. Furthermore, there is excited state absorption (ESA) over the whole spectral window. In the GSB region, the superimposed ESA contribution is immediately noticeable from the positive signal at around 430 nm (probably due to a transition to a higher-lying electronically excited state: $S_1 \rightarrow S_n$). The ESA is much more pronounced to the red (570–770 nm). In this spectral region, one readily observes the beginning of a spectral development, which is due to solvation dynamics caused by the ultrafast reorientation of acetonitrile molecules, which respond to the altered charge distribution when D149 is excited to S_1. This response is reported by the transient red-shift of the SE band of D149.

The solvation dynamics becomes more obvious in the middle panel of Fig. 4, which summarizes the spectral evolution from 0.4 ps to 1.2 ps in 200 fs steps, and from 1.5 ps to 3.0 ps in 500 fs steps. The SE moves further to the red to approach its equilibrium position (compare the steady-state SE spectrum in the bottom panel), and this process results in a negative signal between 650 and 770 nm. At the same time, the superimposed strong $S_1 \rightarrow S_n$ ESA peak centered at *ca.* 600 nm

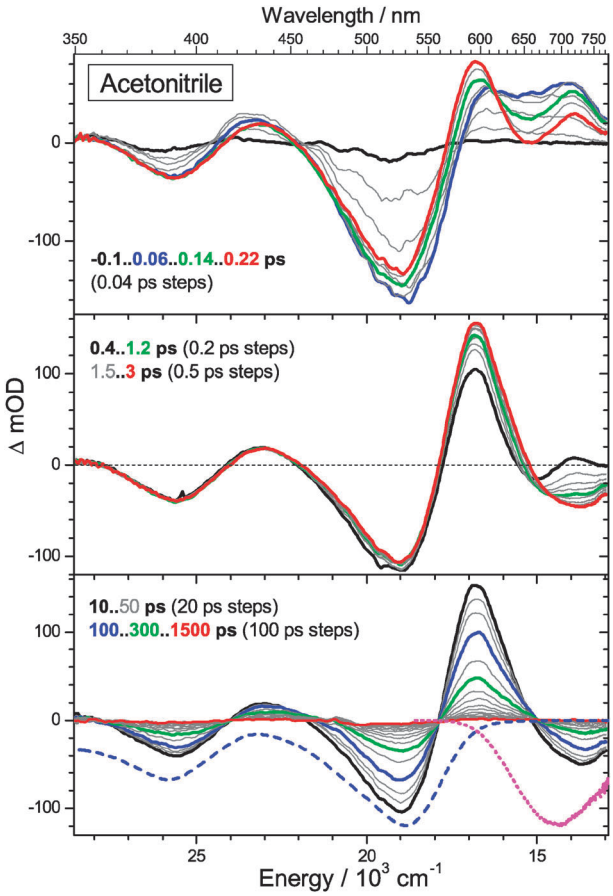

Fig. 4 Transient PSCP absorption spectra of D149 in acetonitrile. Excitation: 476 nm (cross correlation 100 fs): (upper panel) −0.10–0.22 ps with 40 fs steps; (middle panel) 0.4–1.2 ps with 0.2 ps steps and 1.5–3 ps with 0.5 ps steps; (lower panel) 10–50 ps with 20 ps steps and 100–1500 ps with 100 ps steps. Some transient spectra are plotted as thick colored lines for guidance. For comparison, the inverted and scaled steady-state absorption and the scaled steady-state stimulated emission spectrum is shown in the lower panel as blue dashed and magenta dotted lines, respectively.

band rises further up, due to the disappearing SE in that spectral region. The solvation dynamics in acetonitrile have completely ceased by 3 ps, which is the expected timescale in this solvent.[28]

The bottom panel shows the final decay of the $S_1 \rightarrow S_n$ ESA bands and the concomitant filling-up of the GSB with a time constant of $\tau_1 = 280$ ps, which must be dominated by $S_1 \rightarrow S_0$ internal conversion (IC) with a minor contribution of radiative decay. We note that the study of Fakis *et al.* reported a S_1 lifetime of 220 ps in acetonitrile.[14] This is considerably shorter than in our experiments, and is due to the fact that the fluorescence up-conversion transients in that study were measured up to 400 ps, which is too short to determine an accurate S_1 lifetime. In addition to the S_1 spectral decay, we see a barely noticeable change in the ESA band structure, with a time constant of 19 ps. The timescale is consistent with the removal of vibrational excess energy from the S_1 state by collisions with solvent molecules,[20,29,30] but S_1 structural relaxation could be also responsible for this change.

Inspecting the dynamics of D149 in the other two solvents supports the picture outlined above. For methanol (Fig. 5),

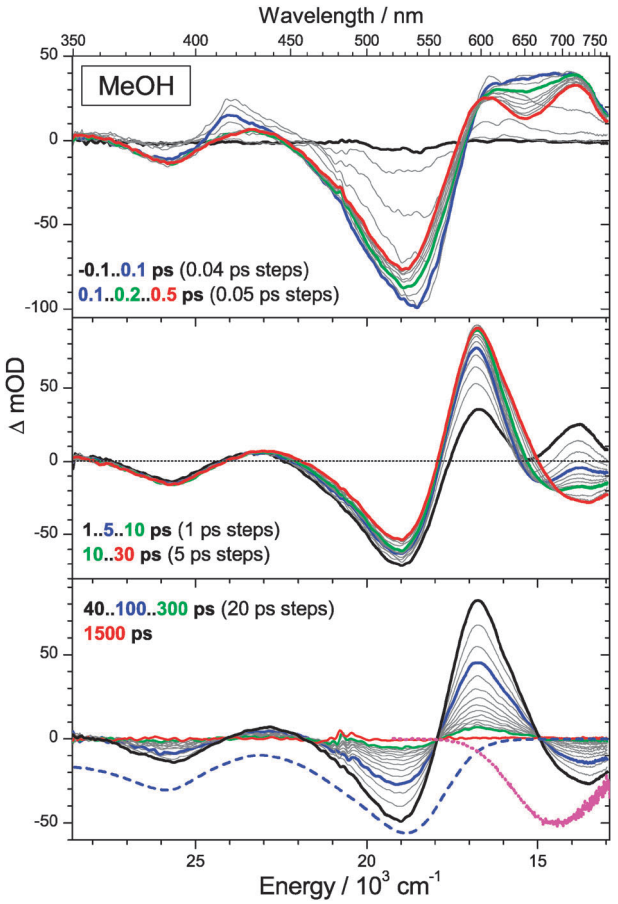

Fig. 5 Transient PSCP absorption spectra of D149 in methanol. Excitation: 479 nm (cross correlation 90 fs): (upper panel) −0.1–0.1 ps with 40 fs steps and 0.1–0.5 ps with 50 fs steps; (middle panel) 1–10 ps with 1 ps steps and 10–30 ps with 5 ps steps; (lower panel) 40–300 ps with 20 ps steps and 1500 ps. Some transient spectra are plotted as thick colored lines for guidance. For comparison, the inverted and scaled steady-state absorption and the scaled steady-state stimulated emission spectrum is shown in the lower panel as blue dashed and magenta dotted lines, respectively. Increased noise around 479 nm (see *e.g.* lower panel) is due to an imperfect stray light subtraction.

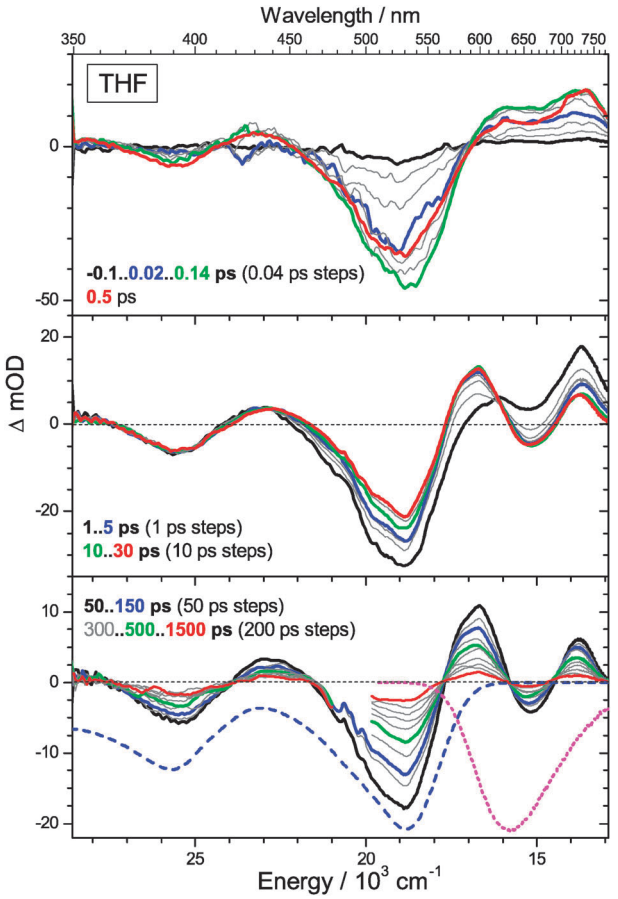

Fig. 6 Transient PSCP absorption spectra of D149 in THF. Excitation: 484 nm (cross correlation 100 fs): (upper panel) −0.10–0.14 ps with 40 fs steps and 0.5 ps; (middle panel) 1–5 ps with 1 ps steps and 10–30 ps with 10 ps steps; (lower panel) 50–150 ps with 50 ps steps and 300–1500 ps with 200 ps steps. Some transient spectra are plotted as thick colored lines for guidance. For comparison, the inverted and scaled steady-state absorption and the scaled steady-state stimulated emission spectrum is shown in the lower panel as blue dashed and magenta dotted lines, respectively. Note that in the bottom panel the wavelength range 480–510 nm has been omitted for a few spectra for the sake of clarity, because there is excessive noise due to an imperfect stray light correction.

the qualitative development is very similar, yet both solvation and $S_1 \rightarrow S_0$ decay proceed on different timescales compared to acetonitrile. Multiexponential solvation dynamics containing fast and slow time constants are found (see the top and middle panels and the global analysis below). Once solvation dynamics has ceased (see the bottom panel which shows clear isosbestic points), the resulting spectrum exhibits SE and ESA band shapes similar to acetonitrile. This is consistent with the comparable Stokes shift of D149 in both solvents, resulting in similar steady-state SE spectra. Interestingly, the lifetime of the S_1 state in methanol is much shorter (τ_1 = 99 ps), pointing toward an acceleration of the IC process, as will be discussed below. Concerning the additional 19 ps ESA dynamics in S_1 found in acetonitrile, it might be also present in methanol. However, it is difficult to separate it from the slowest component of the methanol solvation dynamics which is 11.9 ps.

The data in THF provide an example for D149 relaxation in a mid-polar solvent with fast solvation dynamics (Fig. 6). Again, an ultrafast transient red-shift of the SE is observed in the top and middle panels (which is completed in less than 10 ps), but the spectral appearance is different from that in acetonitrile and methanol, because the Stokes shift in THF is much smaller. The negative SE signal is therefore located more to the blue (negative peak at 660 nm). As a result, the ESA peak at 596 nm is much smaller than in polar solvents, and another ESA peak is visible further to the red, centered at 726 nm, which is otherwise overwhelmed by the more red-shifted SE in polar solvents. The lifetime of the S_1 state is much longer than in acetonitrile and methanol and was independently determined from our TCSPC measurements. A representative trace is shown in Fig. 7, which can be nicely modeled by a clean monoexponential decay with τ_1 = 720 ps. Corresponding TCSPC experiments for D149 in acetonitrile yielded a trace which is slightly wider than the IRF of the TCSPC setup and can be well represented by the decay constant τ_1 = 280 ps from the PSCP experiments. In this case, the time-resolution

Table 2 Summary of global analysis results for D149 in organic solvents

Solvent	λ_{pump}[a]/nm	τ_{CC}[b]/fs	τ_2[c]/ps	τ_1[c]/ps	τ_{relax}[d]/ps	$\tau_{solv,1}$[e]/ps	$\tau_{solv,2}$[e]/ps	$\tau_{solv,3}$[e]/ps
Acetonitrile	476	100	—	280 ± 10	19 ± 10	0.089	0.63	—
	377.5	130	0.4 ± 0.1		—[f]			
Methanol	479	90	—	99 ± 5	—[f]	0.12	0.99	11.9
	377.5	130	0.3 ± 0.1		—[f]			
Ethanol	377.5	130	—	178 ± 10	—[f]	0.39	5.03	29.6
Acetone	377.5	130	—	540 ± 20	—[f]	0.187	1.09	—
THF	484	100	—	720 ± 20	30 ± 10	0.228	1.52	—
	377.5	130	0.6 ± 0.3		—[f]			

[a] PSCP experiment: $S_0 \rightarrow S_1$ excitation at 476–484 nm, UV-pump VIS-probe experiment: $S_0 \rightarrow S_2$ excitation at 377.5 nm. [b] Pump–probe cross-correlation of the experiment extracted from the width of the "coherent artifact". [c] S_2 and S_1 lifetimes τ_2 and τ_1 from transient absorption experiments. In the case of THF the S_1 lifetime of 720 ps was extracted from TCSPC experiments. The corresponding TCSPC value for chloroform is (800 ± 20) ps. [d] Time constant for vibrational relaxation in the S_1 state due to collisions with the solvent (or possibly structural relaxation). [e] Time constants for solvent relaxation taken from ref. 28 (acetonitrile, ethanol, acetone and THF) and ref. 31 (methanol). Note: $\tau_{solv,1}$ for methanol is for a Gaussian function, whereas in all other cases exponential functions are used. [f] Time constant cannot be determined, either due to timescale overlap with $\tau_{solv,3}$ (PSCP, methanol) or due to insensitivity of the transients at 755 nm to this process (experiments with single probe wavelength).

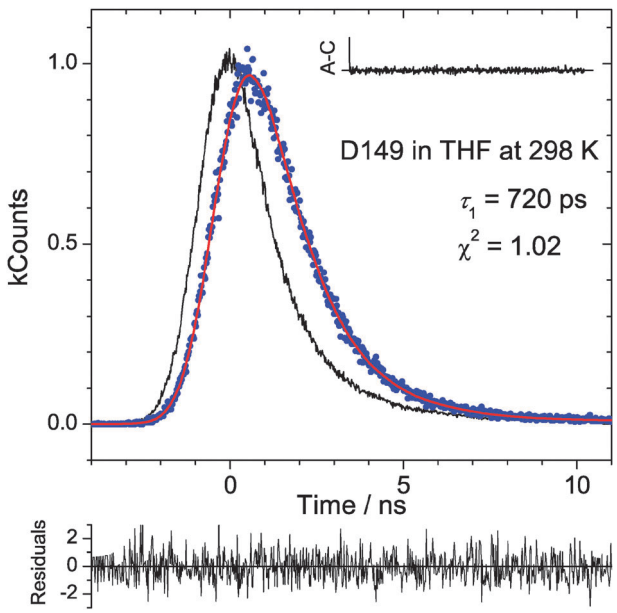

Fig. 7 Time-correlated single photon counting results (blue circles) for D149 in THF at 298 K. Excitation: 337 nm, detection: 610 nm ($S_1 \rightarrow S_0$). The red line is the best fit with τ_1 = 720 ps (χ^2 = 1.02) employing the instrument response function obtained from the scattering solution (black line). The inset shows the autocorrelation (A-C) trace and the lower plot the weighted residuals of the fit.

of the TCSPC setup does not permit an accurate independent determination of τ_1.

3.3 Global kinetic analysis of PSCP data

The transient PSCP spectra in Fig. 4–6 were subjected to a global kinetic analysis based on the simple $S_1 \rightarrow S_0$ model. Solvation dynamics and collisional deactivation of the S_1 state were conveniently modeled by a time-dependent S_1 spectrum, as described in our earlier studies of other molecules.[19,20,30] In contrast to the carotene systems previously investigated by us,[20,30] the influence of vibrationally hot molecules in S_0 on the transient spectra can be safely neglected, because the lifetime of the S_1 state is fairly long compared to collisional relaxation: τ_1 is in the range 99 to 800 ps depending on the solvent, whereas τ_{relax} is *ca.* 19–30 ps (estimate based on the values for S_1). In the case of THF, the decay $S_1 \rightarrow S_0$ is fairly slow, and therefore it cannot be covered completely within the time-window of the PSCP experiments. Therefore the S_1 lifetime was determined from our TCSPC experiments and kept constant in the course of the global analysis.

The resulting time-dependent S_1 spectra for D149 in acetonitrile, methanol and THF are shown in Fig. 8. In all cases, the time-dependence is dominated by the transient Stokes shift of the SE. In contrast, the concomitant shift of the ESA peak at around 600 nm is minor suggesting that the energy gap between the S_1 and S_n states involved in the transition is not changing appreciably in the course of the solvent relaxation. In all cases, the solvation dynamics can be nicely and consistently modeled with the time constants of Horng *et al.* (acetonitrile, THF)[28] and Ernsting and co-workers (methanol),[31] for coumarin 153 and rhodamine 110, respectively. The values are summarized in Table 2: a fast biexponential relaxation in acetonitrile (89 and 630 fs) and THF (228 fs and 1.52 ps) and a more complex response in methanol with one Gaussian and two exponential functions (120 fs, 990 fs and 11.9 ps, respectively). As mentioned above, the additional weak spectral development after completion of the solvent dynamics can be tentatively ascribed to collisional cooling (or possibly also structural relaxation) of the S_1 state, which takes 19 ps in acetonitrile and 30 ps in THF. It might be also present in methanol, however a reliable time constant cannot be extracted due to the overlap with the slowest part of the solvation dynamics.

In Fig. 9, examples for kinetic traces of D149 in methanol are shown for selected wavelengths together with fit results (solid black lines) including the contributions from S_1 (green lines) and S_0 (red lines). The traces at 390 and 500 nm show a steep decay (GSB) and a recovery with a time constant of 99 ps ($S_1 \rightarrow S_0$), with additional weak curvature in the early part of the transients, which is due to solvation dynamics. At 600 nm, $S_1 \rightarrow S_n$ ESA is formed, whereas at 720 nm first $S_1 \rightarrow S_n$ ESA and then $S_1 \rightarrow S_0$ SE develop. In both cases, the final decay is

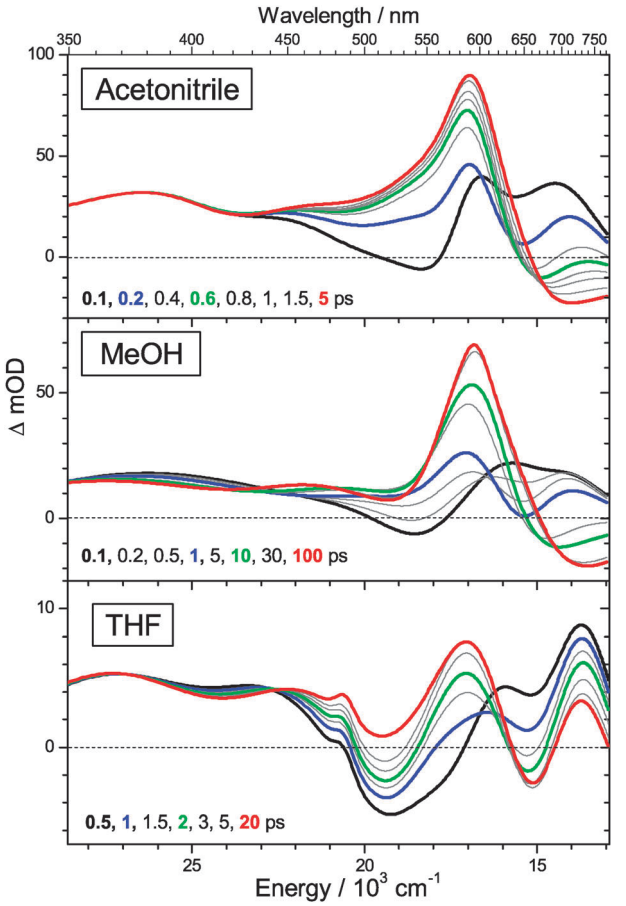

Fig. 8 S_1 spectra of D149 in (A) acetonitrile, (B) methanol and (C) THF as obtained from the global kinetic analysis. The corresponding time for each spectrum is given in each panel.

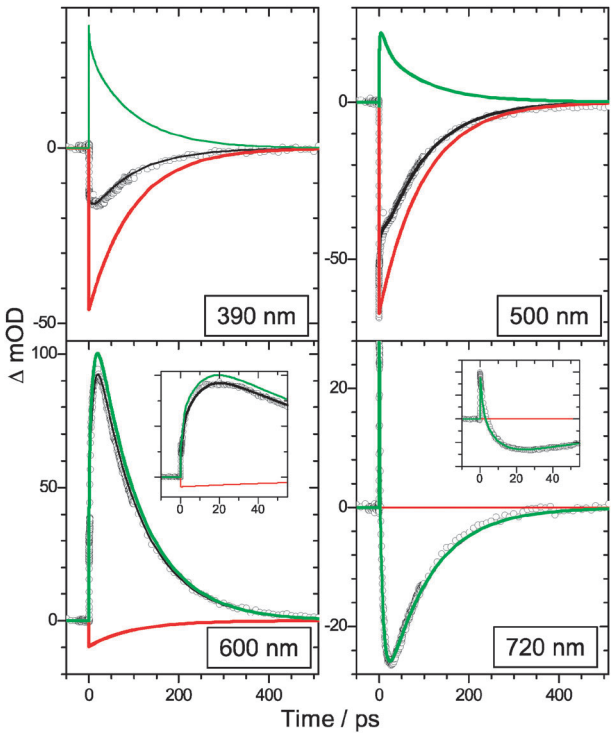

Fig. 9 Kinetic traces for D149 in methanol at four representative probe wavelengths (390, 500, 600 and 720 nm): (circles) experimental PSCP data from Fig. 5; (black line) simulation results from global kinetic analysis with individual contributions from S_1 (green line) and S_0 (red line). In the lower two plots, the insets show magnifications of the transients at earlier times to highlight the curvature in the kinetic traces which is due to solvation dynamics.

also due to the recovery of S_0 with a time constant of 99 ps. The superimposed S_1 solvation dynamics become particularly clear in the insets of the 600 and 720 nm traces, where the magnification shows the characteristic curvature, which arises from the time-dependent Stokes shift of the SE band.

Additional transient absorption experiments have been performed by employing excitation at 377.5 nm ($S_0 \rightarrow S_2$) and probing in the SE band at 755 nm. These experiments will be discussed in more detail in Section 3.4, but at this point we already mention that the measurements in two additional solvents (acetone and ethanol) can also be nicely described by solvation times from the literature.[28] These values are reported in Table 2 together with the S_1 lifetime, which is 178 ps in ethanol and 540 ps in acetone, respectively. Therefore, the lifetime τ_1 of the S_1 state approximately correlates with polarity, *e.g.* acetonitrile (τ_1 = 280 ps) < acetone (τ_1 = 540 ps) < THF (τ_1 = 720 ps) < chloroform (τ_1 = 800 ps). However, interestingly, in protic solvents the lifetime is much shorter [methanol (τ_1 = 99 ps) < ethanol (τ_1 = 178 ps) < acetonitrile (τ_1 = 280 ps)], suggesting a substantial influence of hydrogen bonding on the dynamics. A similar acceleration of nonradiative processes in alcohols was observed for other molecules, such as 4-aminophthalimide.[32] It is accompanied by an increased Stokes shift in protic solvents,[33] which is also observed for D149 (Table 1).

3.4 Lifetime of the S_2 state

In addition to the PSCP experiments employing $S_0 \rightarrow S_1$ excitation we have carried out transient absorption measurements with $S_0 \rightarrow S_2$ excitation at 377.5 nm and single wavelength probing at 755 nm, to determine the lifetime of the S_2 state. An example for the short-time dynamics in methanol is presented in Fig. 10, which contains the transient absorption signals for S_1 excitation (red circles, PSCP) and S_2 excitation (black circles) normalized to the same amplitude of the SE (for both transients occurring at *ca.* 25 ps, not shown here for the sake of clarity). S_2 excitation obviously results in additional $S_2 \rightarrow S_n$ ESA, which is responsible for the increased amplitude at early times. The $S_2 \rightarrow S_n$ ESA decays by $S_2 \rightarrow S_1$ IC to form $S_1 \rightarrow S_n$ ESA, which later on becomes dominated by $S_1 \rightarrow S_0$ SE, once solvation dynamics has sufficiently progressed (compare *e.g.* the 720 nm transient in Fig. 9).

It is obvious that the S_2 lifetime has a critical impact on the appearance of the transient, because it influences the width of the peak, its early-time decay, and (to a much smaller extent) also the signal rise. Using the best fit parameters from the PSCP experiments for methanol in Table 2, the S_2 lifetime and absorption coefficient were simultaneously varied to obtain an optimized fit, which was reached for τ_2 = 0.3 ps (black solid line in Fig. 10). Contributions of S_2 and S_1 to the fit are shown as solid blue and solid green lines, respectively. Shorter (longer) lifetimes result in too narrow (broad) simulations, as shown in the figure. Using a similar approach we obtain a lifetime of

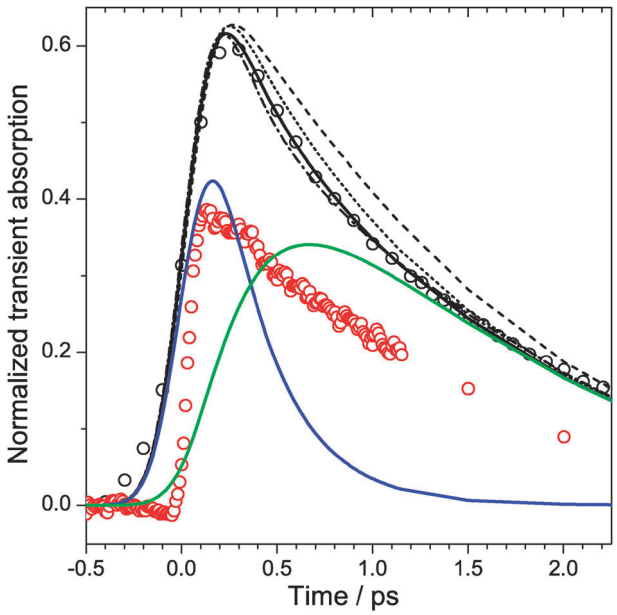

Fig. 10 Comparison of transient absorption profiles of D149 in methanol at 755 nm obtained after S_1 excitation at 479 nm (PSCP, red circles) and S_2 excitation at 377.5 nm (black circles). The black solid line is the best fit for a S_2 lifetime of 0.3 ps, with contributions from S_2 (blue solid line) and S_1 (green solid line). Other black fit lines are from a sensitivity analysis using other S_2 lifetimes: 0.2 ps (dash-dotted line), 0.4 ps (dotted line) and 0.6 ps (dashed line).

0.4 ps in acetonitrile and (less accurate due to a worse signal-to-noise ratio) *ca.* 0.6 ps in THF. Our values are in good agreement with results of Fakis *et al.*, who reported 0.44 ps (toluene) and 0.31 ps (acetonitrile) based on their up-conversion measurements of the S_2 fluorescence.[14]

Our values can be compared with results from another much more approximate indirect approach for obtaining the S_2 lifetime by using the area ratio of the S_2 and S_1 fluorescence bands, which can be estimated from deconvolution of the emission bands in Fig. 3. We note that this deconvolution is not straightforward because the two emission bands overlap. Assuming a simple kinetic scheme involving the nonradiative IC steps $S_2 \rightarrow S_1$ and $S_1 \rightarrow S_0$ as well as the radiative decays from S_2 and S_1 one arrives at:

$$\frac{A_F(S_2 \rightarrow S_0)}{A_F(S_1 \rightarrow S_0)} = \frac{\Phi_F(S_2 \rightarrow S_0)}{(1 - \Phi_F(S_2 \rightarrow S_0))\Phi_F(S_1 \rightarrow S_0)}. \quad (1)$$

In eqn (1) the A_F denotes the areas of the corresponding fluorescence bands. We obtain the area ratio from the deconvolution of the emission bands in Fig. 3(B) as 9.8×10^{-3} in acetonitrile and 6.8×10^{-3} in THF. The fluorescence quantum yield Φ_F for the state S_i is given as

$$\Phi_F(S_i \rightarrow S_0) = \frac{\tau_i}{\tau_{rad,i}}. \quad (2)$$

Here, $\tau_{rad,i}$ and τ_i are the radiative and fluorescence lifetimes for the state *i*. We have roughly estimated the radiative lifetime of the S_2 and S_1 states using the Strickler–Berg formula for the two examples given in Fig. 3.[34] Employing our absorption and fluorescence spectra, an absorption coefficient of 68700 L mol^{-1} cm^{-1} for the maximum of the $S_0 \rightarrow S_1$ band,[2] and wavelength-dependent refractive indices from the literature,[35] we obtain for the S_1 state 6.2 ns in acetonitrile and 4.3 ns in THF. The corresponding values for the S_2 state are 4.3 ns in acetonitrile and 2.7 ns in THF. With D149 in THF, the direct calculation of $\tau_{rad,i}$ from eqn (2) employing the measured Φ_F (0.140 in nitrogen-saturated THF at 298 K) and τ_1 = 720 ps (Table 2) provides a value of 5.2 ns. This confirms that the Strickler–Berg approach provides a reasonable estimate of τ_{rad} for D149. Using these results and our measured S_1 lifetimes τ_1 = 280 and 720 ps in acetonitrile and THF, respectively, we arrive at τ_2 = 1.5 ps in acetonitrile and 3.1 ps in THF. While these time constants suggest a much faster decay of S_2 compared to S_1, they are still substantially larger than our direct determination of τ_2 from transient absorption spectroscopy. This result means that the observed S_2 emission consists in fact mainly of the emission from a small amount of an impurity. This interpretation is also supported by our TCSPC experiments with lamp excitation at 337 nm, where the blue emission band of D149 in THF shows a double exponential decay at 460 nm: the first component has a very small time constant (far below TCSPC time resolution), and the second component is very weak (relative amplitude: 1.9×10^{-4}) and long-lived (decay time constant *ca.* 2.0 ns). The fast and slow components contribute about 30 and 70% to the overall emission intensity at 460 nm, respectively. The TCSPC experiment is practically not affected by photodecomposition due to the very low excitation power (*i.e.* photoproducts are not reexcited). This fact allows us to assign the fast component to S_2 emission of D149 and the long component to the fluorescence of an impurity.

We also note that our experiments employing S_2 excitation suggest the presence of an ultrafast photoinduced process in D149, which must proceed either directly from S_2 or at high excess energies in S_1: for instance, the transient absorption profiles at 755 nm exhibit a small (few percent) residual absorption, which is not present after S_1 excitation (not shown here). In the same experiments, prolonged laser excitation in the S_2 band at 377.5 nm leads to a change in the steady-state absorption spectrum of the solution, where the $S_0 \rightarrow S_1$ band is asymmetrically broadened (reaches further to the red) by a few nm (the exact value depending on the solvent) and, at the same time, the S_2 band reduces in intensity by about 10%. Our reported S_2 lifetime therefore possibly contains contributions from $S_2 \rightarrow S_1$ IC and another nonradiative pathway. Interestingly however, the lifetime of the S_1 state is independent of excitation wavelength. Indications for the formation of a photoproduct are also obtained in experiments with sub-400 nm excitation in the $S_0 \rightarrow S_2$ band of D149 in solution by cw lamp illumination with appropriate filters. In this case, the absorption spectra reach a photostationary state within a few minutes. An example is given in the ESI.† Recall also that the $S_1 \rightarrow S_0$ fluorescence band shows a small red-shift when switching from S_1 to S_2 excitation (Fig. 3(A)). All these observations could be, *e.g.*, tentatively explained by a photoisomerization reaction of D149 after S_2 excitation, yet a full explanation of this complex behavior certainly requires further experiments, which are beyond the scope of the current paper and are currently ongoing in our laboratories.

4. Conclusions

We have presented a comprehensive study of the photoinduced dynamics of the indoline dye D149 in a range of organic solvents. The dynamics after S_1 photoexcitation are fairly simple for such a complex molecule. The increase of the D149 dipole moment upon photoexcitation triggers solvation dynamics on characteristic timescales, which manifest themselves in a transient Stokes shift in the red to near IR region and an accompanying increase of a superimposed prominent ESA band at around 600 nm. The decay of the S_1 state proceeds on a timescale between 99 ps (methanol) and 800 ps (chloroform), and is dominated by internal conversion. In protic solvents, the relaxation is considerably faster than in aprotic solvents of similar polarity, suggesting the influence of hydrogen-bonding, which is likely also responsible for the trends in the Stokes shifts. Transient absorption experiments after S_2 photoexcitation reveal an ultrafast decay of this state on a sub-picosecond timescale and also the formation of a photoproduct, which will require further characterization.

Regarding the already demonstrated successful application of this dye in photoelectrochemical solar cells the following comments can be made: the S_1 lifetime of the "isolated" dye is long enough such that electron injection into semiconductor oxide electrodes (which likely occurs on a 100 fs timescale, possibly with additional picosecond components)[14] should efficiently compete with the intramolecular relaxation of the S_1 state of D149, resulting in a high quantum yield for electron injection. The observed generation of a photoproduct after S_2 excitation is probably not desirable: it might convert the sensitizer into an inactive form, especially under long-term illumination, but in the most favourable case the photoproduct (which has a similar spectrum) might inject electrons as well. Such an unwanted side-reaction could however be efficiently suppressed, once the dye is attached to a semiconductor oxide electrode, as has been demonstrated in the case of merocyanine dyes.[36] Investigations along these lines are currently underway in our laboratories.

Acknowledgements

We would like to thank N.P. Ernsting and J.L. Pérez Lustres for extensive help during the implementation of the PSCP setup, J. Troe and A.M. Wodtke for on-going generous support, as well as R. Bürsing for excellent technical assistance during the experiments. We are also indebted to K.A. Zachariasse for providing his nanosecond TCSPC setup. Finally, we thank M. Takata (Mitsubishi Paper Mills Inc.) and M. Yohei (Inabata UK Ltd.) for discussions on indoline dyes.

Notes and references

1 T. Horiuchi, H. Miura and S. Uchida, *Chem. Commun.*, 2003, 3036.
2 T. Horiuchi, H. Miura, K. Sumioka and S. Uchida, *J. Am. Chem. Soc.*, 2004, **126**, 12218.
3 S. Ito, S. M. Zakeeruddin, R. Humphry-Baker, P. Liska, R. Charvet, P. Comte, M. K. Nazeeruddin, P. Péchy, M. Takata, H. Miura, S. Uchida and M. Grätzel, *Adv. Mater.*, 2006, **18**, 1202.
4 D. Kuang, S. Uchida, R. Humphry-Baker, S. M. Zakeeruddin and M. Grätzel, *Angew. Chem., Int. Ed.*, 2008, **47**, 1923.
5 D. Kuang, J. Brillet, P. Chen, M. Takata, S. Uchida, H. Miura, K. Sumioka, S. M. Zakeeruddin and M. Grätzel, *ACS Nano*, 2008, **2**, 1113.
6 S. Ito, H. Miura, S. Uchida, M. Takata, K. Sumioka, P. Liska, P. Comte, P. Péchy and M. Grätzel, *Chem. Commun.*, 2008, 5194.
7 W. H. Howie, F. Claeyssens, H. Miura and L. M. Peter, *J. Am. Chem. Soc.*, 2008, **130**, 1367.
8 T. Dentani, Y. Kubota, K. Funabiki, J. Jin, T. Yoshida, H. Minoura, H. Miura and M. Matsui, *New J. Chem.*, 2009, **33**, 93.
9 M. Matsui, A. Ito, M. Kotani, Y. Kubota, K. Funabiki, J. Jin, T. Yoshida, H. Minoura and H. Miura, *Dyes Pigm.*, 2009, **80**, 233.
10 N. O. V. Plank, I. Howard, A. Rao, M. W. B. Wilson, C. Ducati, R. S. Mane, J. S. Bendall, R. R. M. Louca, N. C. Greenham, H. Miura, R. H. Friend, H. J. Snaith and M. E. Welland, *J. Phys. Chem. C*, 2009, **113**, 18515.
11 T. Yoshida, J. Zhang, D. Komatsu, S. Sawatani, H. Minoura, T. Pauporté, D. Lincot, T. Oekermann, D. Schlettwein, H. Tada, D. Wöhrle, K. Funabiki, M. Matsui, H. Miura and H. Yanagi, *Adv. Funct. Mater.*, 2009, **19**, 17.
12 U. M. Tefashe, T. Loewenstein, H. Miura, D. Schlettwein and G. Wittstock, *J. Electroanal. Chem.*, 2010, **650**, 24.
13 Y. Selk, M. Minnermann, T. Oekermann, M. Wark and J. Caro, *J. Appl. Electrochem.*, 2011, **41**, 445.
14 M. Fakis, E. Stathatos, G. Tsigaridas, V. Giannetas and P. Persephonis, *J. Phys. Chem. C*, 2011, **115**, 13429.
15 R. Jose, A. Kumar, V. Thavasi, K. Fujihara, S. Uchida and S. Ramakrishna, *Appl. Phys. Lett.*, 2008, **93**, 023125.
16 T. Le Bahers, T. Pauporté, G. Scalmani, C. Adamo and I. Ciofini, *Phys. Chem. Chem. Phys.*, 2009, **11**, 11276.
17 A. L. Dobryakov, S. A. Kovalenko, A. Weigel, J. L. Pérez Lustres, J. Lange, A. Müller and N. P. Ernsting, *Rev. Sci. Instrum.*, 2010, **81**, 113106.
18 T. Lenzer, S. Schubert, F. Ehlers, P. W. Lohse, M. Scholz and K. Oum, *Arch. Biochem. Biophys.*, 2009, **483**, 213.
19 K. Oum, P. W. Lohse, F. Ehlers, M. Scholz, M. Kopczynski and T. Lenzer, *Angew. Chem., Int. Ed.*, 2010, **49**, 2230.
20 K. Golibrzuch, F. Ehlers, M. Scholz, R. Oswald, T. Lenzer, K. Oum, H. Kim and S. Koo, *Phys. Chem. Chem. Phys.*, 2011, **13**, 6340.
21 J. Piel, M. Beutter and E. Riedle, *Opt. Lett.*, 2000, **25**, 180.
22 E. Riedle, M. Beutter, S. Lochbrunner, J. Piel, S. Schenkl, S. Spörlein and W. Zinth, *Appl. Phys. B: Lasers Opt.*, 2000, **71**, 457.
23 M. Kopczynski, T. Lenzer, K. Oum, J. Seehusen, M. T. Seidel and V. G. Ushakov, *Phys. Chem. Chem. Phys.*, 2005, **7**, 2793.
24 M. Kopczynski, F. Ehlers, T. Lenzer and K. Oum, *J. Phys. Chem. A*, 2007, **111**, 5370.
25 U. Leinhos, W. Kühnle and K. A. Zachariasse, *J. Phys. Chem.*, 1991, **95**, 2013.
26 K. A. Zachariasse, G. Duveneck and R. Busse, *J. Am. Chem. Soc.*, 1984, **106**, 1045.
27 *Handbook of Chemistry and Physics*, CRC Press, Boca Raton, 85 edn, 2004.
28 M. L. Horng, J. A. Gardecki, A. Papazyan and M. Maroncelli, *J. Phys. Chem.*, 1995, **99**, 17311.
29 D. Schwarzer, J. Troe, M. Votsmeier and M. Zerezke, *J. Chem. Phys.*, 1996, **105**, 3121.
30 T. Lenzer, F. Ehlers, M. Scholz, R. Oswald and K. Oum, *Phys. Chem. Chem. Phys.*, 2010, **12**, 8832.
31 A. L. Dobryakov, S. A. Kovalenko and N. P. Ernsting, *J. Chem. Phys.*, 2005, **123**, 044502.
32 E. Krystkowiak, K. Dobek and A. Maciejewski, *J. Photochem. Photobiol., A*, 2006, **184**, 250.
33 M. Sajadi, T. Obernhuber, S. A. Kovalenko, M. Mosquera, B. Dick and N. P. Ernsting, *J. Phys. Chem. A*, 2009, **113**, 44.
34 S. J. Strickler and R. A. Berg, *J. Chem. Phys.*, 1962, **37**, 814.
35 C. Wohlfarth and B. Wohlfarth, *Landolt-Börnstein - Vol. III/38, Optical Constants*, Springer, Berlin, Heidelberg, 1996.
36 M. O. Lenz and J. Wachtveitl, *J. Phys. Chem. C*, 2008, **112**, 11973.

